

Simulation of yearly rainfall time series at microscale resolution with actual properties: Intermittency, scale invariance, and rainfall distribution

Nawal Akrour, Aymeric Chazottes, Sébastien Verrier, Cécile Mallet, Laurent Barthès

▶ **To cite this version:**

Nawal Akrour, Aymeric Chazottes, Sébastien Verrier, Cécile Mallet, Laurent Barthès. Simulation of yearly rainfall time series at microscale resolution with actual properties: Intermittency, scale invariance, and rainfall distribution. Water Resources Research, 2015, 51 (9), pp.7417-7435. 10.1002/2014WR016357 . insu-01203278

HAL Id: insu-01203278
https://insu.hal.science/insu-01203278

Submitted on 19 Jul 2020

HAL is a multi-disciplinary open access archive for the deposit and dissemination of scientific research documents, whether they are published or not. The documents may come from teaching and research institutions in France or abroad, or from public or private research centers.

L'archive ouverte pluridisciplinaire **HAL**, est destinée au dépôt et à la diffusion de documents scientifiques de niveau recherche, publiés ou non, émanant des établissements d'enseignement et de recherche français ou étrangers, des laboratoires publics ou privés.

AGU PUBLICATIONS

Water Resources Research

RESEARCH ARTICLE
10.1002/2014WR016357

Key Points:
- Rainfall generator at fine temporal resolution
- Rain support modeling
- Rain events intensity/duration relationship

Correspondence to:
N. Akrour,
Nawal.akrour@Latmos.ipsl.fr

Citation:
Akrour, N., A. Chazottes, S. Verrier, C. Mallet, and L. Barthes (2015), Simulation of yearly rainfall time series at microscale resolution with actual properties: Intermittency, scale invariance, and rainfall distribution, *Water Resour. Res.*, *51*, 7417–7435, doi:10.1002/2014WR016357.

Received 4 SEP 2014
Accepted 28 JUL 2015
Accepted article online 4 AUG 2015
Published online 13 SEP 2015
Corrected 6 NOV 2015

This article was corrected on 6 Nov 2015. See the end of the full text for details.

© 2015. American Geophysical Union. All Rights Reserved.

Simulation of yearly rainfall time series at microscale resolution with actual properties: Intermittency, scale invariance, and rainfall distribution

Nawal Akrour[1], Aymeric Chazottes[1], Sébastien Verrier[2], Cécile Mallet[1], and Laurent Barthes[1]

[1]Université Versailles St-Quentin, CNRS/INSU, LATMOS-IPSL, Guyancourt, France, [2]Sorbonne Universités, UPMC Univ Paris 06, CNRS/IRD/MNHN, LOCEAN-IPSL, Paris, France

Abstract Rainfall is a physical phenomenon resulting from the combination of numerous physical processes involving a wide range of scales, from microphysical processes to the general circulation of the atmosphere. Moreover, unlike other geophysical variables such as water vapor concentration, rainfall is characterized by a relaxation behavior that leads to an alternation of wet and dry periods. It follows that rainfall is a complex process which is highly variable both in time and space. Precipitation is thus characterized by the following features: rain/no-rain intermittency, multiple scaling regimes, and extreme events. All these properties are difficult to model simultaneously, especially when a large time and/or space scale domain is required. The aim of this paper is to develop a simulator capable of generating high-resolution rain-rate time series (15 s), the main statistical properties of which are close to an observed rain-rate time series. We also attempt to develop a model having consistent properties even when the fine-resolution-simulated time series are aggregated to a coarser resolution. In order to break the simulation problem down into subcomponents, the authors have focused their attention on several key properties of rainfall. The simulator is based on a sequential approach in which, first, the simulation of rain/no-rain durations permits the retrieval of fractal properties of the rain support. Then, the generation of rain rates through the use of a multifractal, Fractionally Integrated Flux (FIF), model enables the restitution of the rainfall's multifractal properties. This second step includes a denormalization process that was added in order to generate realistic rain-rate distributions.

1. Introduction

Rainfall is a highly complex, naturally occurring phenomenon, which is extremely variable in both time and space. This variability is the consequence of several characteristics, namely intermittency (rain/no-rain), rain and drought extremes, rain-rate variability, and multiple scaling regimes. One of the challenges of rainfall modeling is that of taking all meteorological scales into account, from the synoptic or mesoscales to the microscale. In recent decades, rainfall modeling has been the focus of an intensive research. However, the modeling of rainfall variability still remains an open topic, especially at small scales. In order to correctly describe natural phenomena, in hydrology in particular, nonlinear dynamic models are needed. In this perspective, it is crucial to improve the fine-scale modeling of rainfall events, in order to take this fine-scale information correctly into account.

In this context, several stochastic models have been proposed. The modeler must initially decide whether rainfall will be viewed as a continuous or discrete process; in this context a more thorough review of rain models can be found, for example, in *De Michele and Ignaccolo* [2013]. Once this choice has been made, various approaches can be used. For example *Cooley et al*. [2007] proposed a Bayesian hierarchical model to characterize extreme precipitations events produced by a regional climate model. *Wang et al*. [2012] chose to infer dry and wet periods using Markov switching models. A large number of rainfall generators are based on a pulse/point Poisson process, among others [*Onof et al*., 2000; *Burton et al*., 2008; *Evin and Favre*, 2013; *Bernardara et al*., 2007]. Geostatistical techniques such as kriging have been used to model rainfall [*Schleiss et al*., 2009, 2014; *Leblois and Creutin*, 2013], and other types of model, such as that of *Tyralis and Koutsoyiannis* [2011], based on a Hurst-Kolmogorov model, have also been used. Among these numerous models, multifractal approaches, especially the Universal Multifractal [UM] one [*Schertzer and Lovejoy*, 1987,

1991; *Deidda et al*., 1999; *Deidda*, 2000] have received a great deal of attention in the geophysical literature. Based on an observed scale invariance property called multifractality, these models use the concept of either discrete or continuous multiplicative cascades [e.g., *Schertzer and Lovejoy*, 1987; *Lovejoy and Schertzer*, 1995; *Lovejoy et al*., 2008; *Lovejoy and Schertzer*, 2010; *Serinaldi*, 2010; *Gaume et al*., 2007].

Among the various approaches used to reproduce different scale invariance regimes through the concept of multiplicative cascades, two of these methods are generally applied. The first of these is the "bottom-up" approach, in which the simulation process focuses on the finest scale in an attempt to converge toward large-scale fractal behavior (i.e., from finer to coarser scales). The second is the "top-down" approach, in which the simulation process goes from coarser resolutions to finer resolutions, through the use of fractal cascades to achieve successive downscaling steps. In this case, the rain support could be obtained simply by applying a very small threshold. In practice, rain intermittency is not adequately handled by basic Universal Multifractal (UM) models. As it will be explained in section 3.4, these models are not designed to generate zero values. Various approaches have been investigated, to solve the problem of simulating zero values [*Olsson*, 1998; *Gires et al*., 2013; *Schmitt et al*., 1998]. Several researchers have introduced beta components, i.e., a simple on/off cascade model, in the generation process (see *Schertzer et al*. [2002] for further details). The beta-log-stable process generalizes most of the multifractal scaling models proposed for rainfall simulation. These are also referred to as beta-lognormal or beta-log-Levy models, depending on whether the stability parameter α is equal to, or is strictly smaller than 2 [e.g., *Over and Gupta*, 1996; *Serinaldi*, 2010; *Veneziano et al*., 2006; *Veneziano and Lepore*, 2012]. Although this model allows zero values to be generated, it does not provide realistic rain/no-rain durations [*Schmitt et al*., 1998]. The generalization of this process to continuous cascades, as proposed by *Schmitt* [2014], provides a more realistic modeling, but it is not able to correct the model's intrinsic inability to simulate realistically both dry and wet periods.

Although some of the proposed models are able to simulate the multiple scaling regimes (and coherent multifractal properties) of rain observations [e.g., *Hubert*, 2001; *Lovejoy and Schertzer*, 2010; *Schertzer and Lovejoy*, 2011; *Serinaldi*, 2010], the simulation must reproduce the scaling properties of the three meteorological scales (i.e., synoptic scale, mesoscale, and microscale). These models thus fail to provide simulations that are fully representative of measured rain data, especially to represent correctly all of these scaling regimes (as well as the transitions in between). Furthermore, the statistical distribution of the simulated rain-rate series is not consistent with those directly estimated from rain gauge measurements [e.g., *Hubert*, 2001].

Another important aspect is the nature of the data set used to build the model. Since large rainfall databases have been created throughout the world, most rain models were developed from rain gauge data with a daily or hourly temporal resolution. Although, as pointed out by *Rupp et al*. [2009], an interesting way to generate fine-scale rainfall on the basis of coarser scale historical records or long-term forecasts is to stochastically disaggregate rainfall from coarser to finer scales, this approach is not considered here. Indeed, in section 4, it is shown that with a (sufficiently long) high-resolution data set, the rain support and average rain rate of the time series used in the present study (see section 2) require specific modeling for periods of time shorter than 5 min. As explained by *Veneziano and Lepore* [2012] and *Gires et al*. [2013], the simulation of the rain support is crucial, when rainfall time series need to be simulated with scaling properties. These observations suggest that the straightforward disaggregation of rain gauge time series may not be a well-adapted approach.

The simulator developed in the present study is based on the sequential simulation of rain support and intrarain/within-rain variability, using an approach similar to that of some previously cited studies [*Schleiss et al*., 2014; *Leblois and Creutin*, 2013]. The rain support is considered as a sequence of alternating, independent periods of rain/no-rain. These generated using two different Pareto laws, proposed in the study of *Lavergnat and Golé* [1998, 2006] who studied rainfall by analyzing rain droplets. When the rain support is considered to be the result of a two-state renewal process, a simulation of intrarain/within-rain events is required.

In order to generate realistic rainfall time series over a wide range of scales, namely from 15 s to 1 year, we have developed an approach based on a continuous, multiplicative cascade model. Following the concepts proposed by *De Montera et al*. [2009] and *Verrier et al*. [2011], the scaling properties of the rain rates are simulated, through the use of parameters estimated from fine-scale observations. For this, we adopted the

multifractal Fractionally Integrated Flux (FIF) model, which simulates a log-stable stochastic process, based on the Universal Multifractal (UM) model developed by *Schertzer and Lovejoy* [1987].

The aim of this study is to address (and solve) some of the main drawbacks of the model proposed by *De Montera et al*. [2009]. The latter uses a thresholded multifractal FIF model, in which intermittency is introduced by applying an appropriate threshold to the time series. The goal is to assess the main properties of a measured time series, given a limited number of parameters. The improvements proposed here are designed to provide a more realistic simulation, reproducing various important statistical properties of rainfall, in particular its variability, intermittency, and power spectrum, while maintaining a consistent rain-rate distribution at different time scales. As could be expected, these improvements are achieved at the cost of increased complexity in the modeling of realistic rain events.

This paper is organized in six parts. Following the introduction, section 2 presents the data set and its specificities. In section 3, the hypotheses on which the simulator is based are described in detail. For each hypothesis presented in section 3, section 4 provides the corresponding formulation and parameters. Each subsection highlights the coherence between the measured and simulated data series. At the end of section 4, the complete simulation process is summarized. Section 5 discusses the simulator's accuracy, together with various results in support of our initial hypotheses. We thus show that by aggregating the simulated fine-resolution time series, a coarser time series can be retrieved, which is consistent with the aggregated, measured time series. We also demonstrate the ability of the simulation process to reproduce various scaling regimes over the full time series. Our conclusions, together with possible perspectives, are discussed in the last section.

2. The Data Set

This study relies on the use of rain-rate (hereafter RR) time series obtained using a disdrometer (more specifically a Dual-Beam Spectropluviometer, hereafter DBS), described in detail by *Delahaye et al*. [2006]. This instrument allows the incoming droplets passing through its capture area to be monitored in terms of their arrival time, diameter, and fall velocity. Each drop is time stamped with an accuracy of 1 ms, thus ensuring good temporal resolution for rain support retrieval. As the capture area of this sensor is a 100 cm^2 rectangle, observations of the rainfall process are extremely localized. The collected drops are then analyzed to estimate the corresponding rain rate, with an integration time of 15 s. Rain studies are highly dependent on the sensor used for rain-rate acquisition, and all data-based models rely on its given resolution, accuracy, and detection threshold. As a consequence, there are almost as many rain models (and in particular, as many parameter sets) as there are types of sensors. Even if they are different, these various sets of parameters may be consistent, such that the simulations obtained with them can have similar properties. Hence, they may be used to reproduce rain-rate series observed at various resolutions, or measured with various accuracies.

Following *De Montera et al*. [2009], the 15 s time resolution was determined from the quality of the scaling restitution. The limits of the power spectrum scaling range are studied, because they indicate the maximum and minimum scales over which it is meaningful to perform multifractal analysis. In the case of the present measurements (not shown here), the spectrum clearly levels off at frequencies above 1/30 Hz, such that the time series must be averaged over 15 s time lags in order to retain the scaling component of the power spectrum only.

In the present study, we have used a data set made up from two time series. The first of these, used as training data, was recorded over a 2 year period (July 2008 to July 2010), and the second (used only in section 5 for validation) was recorded over a period of 2 years and 7 months (from October 2010 to June 2013) at the "Site Instrumental de Recherche par Télédétection Atmosphérique" (SIRTA) in Palaiseau, France. Since the DBS detects droplet velocities, it can easily distinguish between rain and snow, due to considerably lower velocity of snowflakes. Snowy episodes, as well as outliers, were thus removed from the data during the preprocessing of the rainfall time series. As previously described, the properties of the observed rain-rate time series, depend on the one hand, on the sensor's temporal resolution, and on the other hand, on its rain-rate detection threshold. A high detection threshold may overlook weak rain events, and thus overestimate the length of dry periods (hereafter, referred to as no-rain durations). Conversely, a low threshold may not discard small isolated "false detection" raindrops resulting from dust or insects, leading to an underestimation

of the duration of dry periods. In the case of the DBS series, the sensing threshold was set to 0.05 mm h^{-1} (for a 15 s integration time), thus ensuring that both the estimated rain support and rain-rate measurements are accurate. Finally, the training data series (resp. validation data series) is composed of 5.2×10^6 samples (resp. 7.6×10^6) recorded with a 15 s resolution (i.e., rain rates integrated over a 15 s time span). In this data set, 4.6% (resp. 5.3%) of the samples are rainy samples, corresponding to more than 1000 h of rain (resp. 1670 h), distributed over 12, 195 (resp. 18, 840) continuous wet periods. Some of the rain events included in the training time series had been used in previous studies [*Verrier et al*., 2011], to analyze the scaling properties of rain at a fine temporal scale, by implementing a slightly different preprocessing technique.

3. From Modeling Toward Simulation

3.1. Introduction

Different studies have shown that rain-rate time series have multiple scaling regimes. In *Verrier et al*. [2011], multifractal analysis of high-resolution data showed that two multiscaling regimes (with different UM parameters) could be distinguished, i.e., from 3 days to 32 min and from 16 min to 15 s. The former is likely to represent interevent variability, whereas the latter is likely to represent the internal variability of a single event (hereafter, referred to as within-rain variability). The position of the break between the two scaling regimes is directly related to the characteristics of the support. Thus, as described by *De Montera et al*. [2009], *Veneziano and Lepore* [2012], and *Gires et al*. [2012], multiscaling parameters of entire rain time series are found to strongly depend on the rain support characteristics. An event within-rain variability could be perceived as being governed by the laws of atmospheric fluid mechanics [*De Montera et al*., 2010; *Lovejoy and Schertzer*, 2008]. Thus, as explained in *Verrier et al*. [2010] and *De Montera et al*. [2009, 2010], consistent values of the UM parameters (resulting from an event within-rain variability) can be expected, in both the spatial and time domains anywhere in the world. The classical (meteorological) definition of rain events includes small values, with relatively short zero periods inside events. These notions are inevitably conditioned by the characteristics of the sensor. Indeed, conventional rain gauges measure integrated quantities and do not allow the transition between rain and no-rain periods to be clearly distinguished. As DBS measurements accurately measure the arrival time of each drop, they make it possible to determine whether or not it is raining within time periods 15 s each. The approach presented in this study is based on the use of DBS measurements, and thus calls for a clear definition of the entangled notions of rain and no-rain events. Here we do not use the classical definition of rain events, but rather the notion of a "continuity" of rain and no-rain periods. To avoid confusion, the term "period" is used in the following. In this context, a "no-rain period" is a series of consecutive, null 15 s rain rates, characterized by their duration d_{nr}. Similarly, a "rain period" will correspond to a series of consecutive, nonnull, 15 s long rain interval. Each "rain period" is characterized by its duration d_r, that is, the number of consecutive 15 s non zero rain-rate intervals and its corresponding average rain rate $\langle RR \rangle$, which is the average value of the continuous rain rates RR (integrated over 15 s) belonging to the same "rain period."

3.2. Main Assumptions

Our simulator was designed on the basis of three main assumptions. The first of these is related to the rain support, whereas the other two are related to the internal properties of rain. The validity of these assumptions with respect to our data sets is discussed in the following (sections 4 and 5).

Assumption 1: Adopting the findings of *Lavergnat and Golé* [2006] and *Schmitt et al*. [1998], we consider the rain support to be a sequence of alternating (and independent) rain d_r and no-rain d_{nr} durations.

It is important to note that, in the meteorological sense, whether it be convective or stratiform, a rain event is disaggregated into several rain periods that are likely to be governed by the same dynamics. In accordance with the notions proposed by *De Montera et al*. [2009] and *Gires et al*. [2013], in the present study, we use the same mean multifractal parameters for all rain periods. Furthermore, we assume that these periods differ mainly in terms of their average rain rates $\langle RR \rangle$.

Assumption 2: The rain's multifractal behavior occurs within-rain periods, and the FIF model is thus used to generate rain periods, one rain period at a time. In addition to this hypothesis, we consider the rain's scaling properties to be stationary and independent of the rain period.

Thus, for each rain period, the FIF model makes it possible to generate normalized rain rates RR_N. A denormalization step is then needed, in order to simulate actual rain rate RR time series.

Assumption 3: To simulate actual rainfall, we assume that, for each rain period, there is a relationship between the rain duration d_r (resulting from the support simulation) and the corresponding average rain rate $\langle RR \rangle_{d_r}$.

Since the duration of a rain period, d_r, is known when its average rain rate $\langle RR \rangle$ is drawn, we can also use the notation $\langle RR \rangle_{d_r}$ to emphasize the rain rate's dependence on the assumed value of rain duration d_r (assumption 3). Thus, the *RR*s are obtained by multiplying the normalized RR_N values with respect to the average rain rate $\langle RR \rangle_{d_r}$.

3.3. Rain Support Model (Assumption 1)

When the rain rates are thresholded at a given resolution, the support can be considered to behave as a Boolean process. Here since we are dealing with a one dimensional problem, and it is assumed that the rain duration d_r and the no-rain duration d_{nr} are two independent random variables, we can simply draw consecutive (and alternating) rain d_r and no-rain d_{nr} durations. Using the definition of rain/no-rain durations given at the end of section 3.1, our definition for rain support is based on the presence or absence of a rain droplet over a time span of 15 s.

Using a disdrometer, allowing accurate time stamping of raindrop times of arrival, *Lavergnat and Golé* [1998] were able to separate interdrop arrival times into two classes: less than 5 min, and more than 5 min. As a consequence, no-rain durations d_{nr} could also have two different behaviors: one prevailing over periods of less than 5 min, and the other characterized by periods longer than 5 min. Similarly, a rain duration d_r can have two prevailing behaviors, i.e., less than and more than 5 min [see *Lavergnat and Golé*, 2006, Appendix A]. According to *Lavergnat and Golé* [2006], the distribution of rain/no-rain durations is very close to a Pareto distribution.

3.4. Modeling Within a Single Rain Period (Assumption 2)

The core of the rain simulator is a time series generator, based on the implementation of multifractal theory [*Schertzer and Lovejoy*, 1987], which is characterized by scale invariance properties complying with those observed on continuous rain-rate time series. It is commonly accepted that rain can be described in a multifractal framework. When, introduced into the turbulence theory, multiplicative cascades [*Novikov and Stiuart*, 1964; *Yaglom*, 1966] were the conceptual tool used to model stochastic processes and fields having a multifractal behavior. They are defined by hierarchical and iterative methods, which allow the appropriate quantity of energy to be determined at a finer resolution λ_n, on the basis of the energy known at a given initial (coarser) resolution λ_1. Such a cascade is constructed from a large scale, down to smaller scales. After $n-1$ steps, the transition from resolution λ_{n-1} to resolution λ_n is obtained from equation (1):

$$\Phi_{(n,i)} = \Phi_{(n-1,j)} \mu\phi_{(n,i)} \tag{1}$$

where the positive field at resolution λ_{n-1} is denoted by $\Phi_{(n-1,j)}$, $j = 1, \ldots, 2^{n-1}$ is the time index of the cascade process, and i is the time index at the next resolution step. For a given value of j, i has two possible values ($i=2j-1$ and $i=2j$).

Multiplicative cascades Φ are composed of a series of random variables $\mu\phi_i$ referred to as "multiplicative increments," which are generally assumed to be independent and identically distributed. A discussion of this multifractal model hypothesis is provided in *Veneziano et al*. [2006] and *Serinaldi* [2010]. As the fields generated by such models are scale-invariant multiplicative cascades are widely used to build multifractal fields [*Schertzer et al*., 2002]. It is generally assumed that the mean value of the process is statistically preserved, regardless of the resolution λ: $\forall\lambda, \langle\Phi_\lambda\rangle = M$ (where $M = 1$ in the present case). Whatever the resolution, the statistical properties of the cascade are characterized by a moment scaling function $K(q)$:

$$\forall q, \langle \Phi_\lambda^q \rangle \propto \lambda^{K(q)} \tag{2}$$

where $\langle . \rangle$ is the averaging operator and q is the order of the moments. In the context of the Universal Multifractal (UM) models proposed by *Schertzer and Lovejoy* [1987], the moment scaling function is defined by two parameters only, α and C_1:

$$\begin{cases} K(q)=\dfrac{C_1}{\alpha-1}(q^{\alpha}-q) & \text{if } \alpha \neq 1 \\ K(q)=C_1.q.\ln(q) & \text{if } \alpha = 1 \end{cases} \quad (3)$$

where α represents the multifractality parameter and can have values between 0 (monofractality) and 2 (log-normality). C_1 provides a measure of the inhomogeneity of the mean level of the field, and for a D-dimensional process, it lies in the interval $[0, D]$.

Contrary to UM fields, most geophysical data are nonconservative. From a conservative UM field Φ_λ, the Fractionally Integrated Flux (FIF) model [*Schertzer and Lovejoy*, 1991; *Schertzer et al*., 2002; *Pecknold et al*., 1993] computes a nonconservative field noted $\Phi_\lambda \Delta t^H$, through a fractional integration of order H. The fractional integration parameter H is referred to as the nonconservative parameter. This additional parameter is equivalent to the Hurst exponent and leads to the following statistics for the nonconservative field increments:

$$\langle (\Phi_\lambda \Delta t^H)^q \rangle \sim \lambda^{-\zeta(q)} \quad (4)$$

where Φ_λ is the conservative field at resolution λ, Δt is the time increment ($\Delta t = \frac{T}{\lambda}$), T is the length of the time series, $\langle . \rangle$ denotes the averaging operator, and $\zeta(q)$ is the exponent of the FIF structure function of order q which is given by *Vainshtein et al*. [1994]:

$$\zeta(q)=qH-K(q) \quad (5)$$

The structure function can be used to determine the parameter H. For more details concerning the properties of UM and FIF models, see *Schertzer et al*. [2002] and *Schertzer and Lovejoy* [2011].

Although a FIF model implies long-range dependence, given assumption 2, this dependence is valid during rain periods only. The FIF model has just one scaling regime and is thus ideal for the modeling of stochastic processes with scaling properties, provided no zero values are involved. Thus, as in *De Montera et al*. [2009], and as discussed in *Veneziano and Lepore* [2012], the multifractal parameters were estimated on a per rain period basis (since we work with rain periods rather than events). By working with consecutive, nonnull 15 s rain rates, during rain periods, we ensure that we are working "within rain," and that the properties and parameters estimated using the rain rates (integrated over 15 s) are not biased by the rain support. The multifractal parameters therefore correctly reflect the variability occurring within a given rain period and not that corresponding to the rain support. As assumed by *Verrier et al*. [2011], and mentioned by *Gires et al*. [2013] and *Veneziano and Lepore* [2012], we believe that the many parameter sets reported in the literature can be largely explained by the fact that they result from a mixture of "within rain" and "rain support" variabilities. Just as it is consistent to estimate a set of FIF model parameters corresponding to each separate rain period, it should also be consistent to simulate the rain-rate time series in the same manner.

3.5. Multifractal Denormalization Within a Rain Period (Assumption 3)

The FIF model is basically a multiplicative cascade, based on the use of ratios. It allows the simulation of time series with accurate scale properties but not with actual rain-rate time series, since the UM model works with the relative values RR_N (introduced previously) such as $\langle RR_N \rangle = 1$. Here, the denormalization is carried out, rain period by rain period, at the smaller scale. We thus denormalize each simulated rain period separately.

Once the rain support (and therefore the rain durations) is known, we can "denormalize" each rain period relative values RR_N to obtain correct rain rates RR. More precisely, each rain period is denormalized by multiplying the RR_N by an average rain rate $\langle RR \rangle_{d_r}$ drawn according to its duration d_r. By considering the duration d_r only, when retrieving $\langle RR \rangle_{d_r}$, we discard a certain degree of seasonal variability. Since rain events can be viewed as a succession of quiescent and active phases [*Ignaccolo and De Michele*, 2010], the disaggregation of events into rain periods emphasizes the heterogeneity of rain and therefore weakens the seasonal information contained in the original data. This preference is discussed in section 4.3 in which the corresponding value of $\langle RR \rangle_{d_r}$ is characterized by a random variable.

4. Parameterization of the Simulator

As previously explained, the primary aim of this study is to develop a methodology allowing realistic, synthetic rain-rate time series to be generated over a wide range of scales, i.e., to conserve the statistical

Table 1. Percentage of Short Durations Used to Simulate the Rain Support (Column 2) and the Fitted Pareto Parameters (Columns 3–8)

	Probability to Have Short Durations: $Pr(d < 5\,\text{min})$	Pareto Parameters for Short Durations			Pareto Parameters for Long Durations		
		K	σ	θ	K	σ	θ
No-rain durations	0.78	1.56	0.32	0.25	1.88	14.35	4.75
Rain durations	0.87	1.79	0.31	0.25	0.74	7.77	4.75

properties of within-rain periods, while correctly taking the existence of rain and no-rain durations into account. In order to implement this methodology, the various laws and parameters of the proposed simulator (Pareto law for the rain support, multifractal parameters for the within-rain period, and a law further defined for within-rain period denormalization) are estimated based on the training time series described in section 2.

4.1. Rain Support Simulation Parameters (Assumption 1)

The rain support modeling described here is derived from a previous study of *Lavergnat and Golé* [1998, 2006]. These authors observed that the distribution of interdrop time intervals "suggests that the arrival of raindrops may be governed by a point renewal process," and found that the correlation coefficient between two consecutive arrivals is 0.08. From the data set used, in the present study, we are able to confirm some of these properties. Visual analysis of the joint distribution between two consecutive rain no-rain durations (not shown) shows that these two variables are indeed independent. This is confirmed by the very low correlation coefficient, of 0.003. This result makes it possible to simulate the rain support as a succession of independently drawn, alternating periods of rain and no-rain (assumption 1). For each rain d_r and no-rain d_{nr} duration, we first need to randomly draw whether it is a short or a long duration (cf. second column of Table 1). The simulated short/long durations, d_r and d_{nr}, are then drawn from a Generalized Pareto law (characterized by equation (6)) using parameters estimated from measured values of d_r and d_{nr}.

$$f(d/k,\sigma,\theta)=\left(\frac{1}{\sigma}\right)\left(1+k\frac{(d-\theta)}{\sigma}\right)^{-1-\frac{1}{k}} \tag{6}$$

where d denotes the duration, i.e., short or long d_r or d_{nr}. k, σ, and θ are the shape, scale, and location parameters, respectively, of the generalized Pareto probability density function. Since the rain intensities are estimated over a 15 s duration, the durations have discrete values. As described in section 2, their distribution is discretized at 15 s intervals, corresponding to the integration time chosen for the calculation of the rain rate. Accordingly, the same discretization is used when simulating the durations. Table 1 shows the Generalized Pareto-distribution parameters estimated from measured, short/long rain/no-rain durations. The location parameter, θ, for long durations is set to 4.75 min, since the minimum value of a long duration has to be greater than or equal to 5 min and 0.25 min, i.e., 15 s, fort short durations.

The normalized histograms of the simulated rain/no-rain durations are shown in Figure 1. According to our hypothesis, the good agreement between measured and simulated durations leads to a correctly simulated rain support. For each distribution, this is confirmed by a two-sample Kolmogorov-Smirnov test, which does not reject the null hypothesis, with a 99% level of confidence. To highlight this aspect, in section 5.1, it is shown that the scaling properties of the measured series are relatively well simulated.

4.2. Within-Rain Period RR_N Simulation Parameters (Assumption 2)

The FIF model used to simulate the normalized values of a rain period RR_N is described in section 3.4. This generator was derived from the simulator of *Lovejoy and Schertzer* [2010] which is freely available on the Internet (www.physics.mcgill.ca/ ~gang/software/). The generator requires three previously defined parameters H, α, and C_1. We recall that a rain period does not correspond to a real rain event, but rather to consecutive rain-rate values exceeding a certain threshold (see the end of section 3.1). The development of an appropriate methodology for the determination of the multifractal, time-domain properties of rain has been discussed in many studies [e.g., *Pathirana et al*., 2003; *Molini et al*., 2009; *De Montera et al*., 2009]. In particular, *Verrier et al*. [2011] who use a portion of the same data set as the one used here, investigate the scaling properties of a high-resolution data set within the framework of Universal Multifractals. In this study, different approaches (continuous events and continuous series) are compared, the effect of the rain support

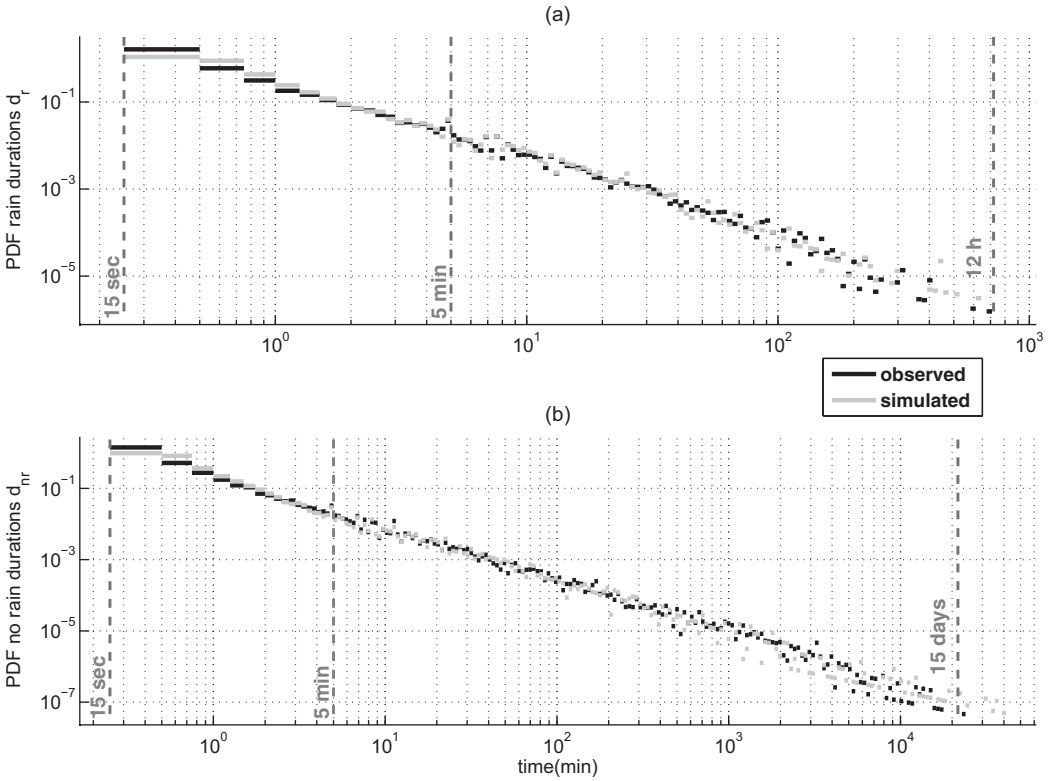


Figure 1. Estimated probability density function for (top) rain durations d_r and (bottom) no-rain durations d_{nr}, for the training measured time series (black) and the simulated time series (grey). Both time series have the same length equal to 2.5 years.

is discussed, and semitheoretical formulae are proposed for the bias introduced by the support zeros. The aim of the present study is not to develop the analysis methodology itself but, rather to demonstrate the simulator's ability to reproduce realistic rain properties. We use the same methodology as that of *Verrier et al*. [2011], which is implemented rain period by rain period, in order to estimate the corresponding parameters.

According to *Tessier et al*. [1996], the fractional integration parameter H can be estimated by fitting the first-order structure function. From the latter study, it could be conjectured that the rain process is nonconservative at small scales, between 1 min and about 30 min [see *Verrier et al*., 2011, Figure 8]. The study of the first-order structure function was used to infer the parameter H corresponding to our data set. A break of the first-order structure function is observed around 32 min. It allows the retrieving of $H \sim 0.4$ for scales that are shorter than 32 min. To check the consistence of the model, the mean value of the parameter H was estimated over 32 –min long simulated rain periods. The corresponding value was found to be 0.44, which was considered sufficiently close to the value 0.4 retrieved from observed rain-period data.

In order to estimate the parameters α and C_1, a classical procedure for the investigation of multifractality (the Trace Moments method) was applied to the differentiated series $(|\Delta RR_N|)$ [*Lavallée et al*., 1993]. For each rain period, the moment scaling function $K(q)$ was estimated for several given orders q (16 linearly spaced values going from 0 to 1.5). For each order q, the value of $K(q)$ was computed thanks to a power law fitting of equation (2) (as a function of the resolution λ). Given this set of points, the α and C_1 parameters were then inferred by a mean square fit of the function $K(q)$ given in equation (3) (see *Tessier et al*. [1993] for details). This estimation was restricted to rain periods lasting strictly more than 12 min. Since some rain periods did not display scaling, we limited the α and C_1 estimation to rain periods satisfactorily in agreement with equation (2). This was done by keeping only the rain periods having an average R^2 (of the power law fittings) greater than 0.8. Hence, 9% of the remaining rain periods were discarded.

Although the variation of the estimated parameters α and C_1 was studied as a function of the rain duration d_r, this did not produce any significant results. As a result of the lack of long rain-duration data in our time

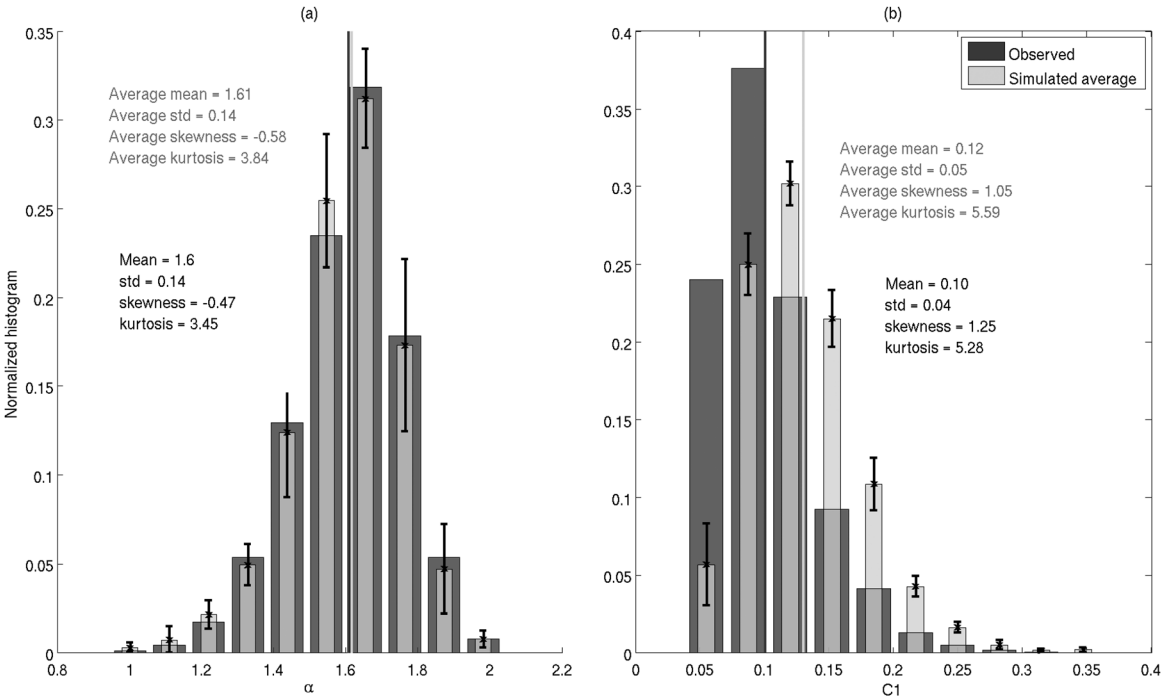


Figure 2. Fluctuations of (left) α and (right) C_1, estimated for all rain periods extracted from the training measured time series (dark grey), and fluctuations of α and C_1 (light grey), estimated for a thousand simulated time series of the same length, where $\alpha=1.6$ and $C_1=0.1$. For each bin of the histograms, the error bar corresponding to a standard deviation is also displayed.

series, it is difficult to determine whether there is a relationship between these parameters. The histograms of the parameters estimated from the observed data (the training 2 year long measured time series presented in section 2) are shown in Figure 2. The values of the Fractionally Integrated Flux (FIF) parameters, α and C_1, were obtained from our data set as the average of the estimated values, taken over all of the rain periods, that is, 1.6 for the parameter α and 0.1 for the parameter C_1. These values are consistent with the parameters estimated in the literature, using similar methodologies. Using this approach, *Pathirana et al.* [2003] estimated the values of α to lie between 1.09 and 1.92, whereas the value of C_1 was found to lie in the range between 0.26 and 0.42, for several time series. *De Montera et al.* [2009] found $\alpha=1.69$ and $C_1=0.13$, and *Rodríguez et al.* [2013] estimated $\alpha=1.23$ and $C_1=0.14$. There is currently no consensus as to the characteristic parameters of multifractality, and it is not possible to know whether the differences in the values found by various authors are due to the methodologies they adopted, the sensor's characteristics or the natural variability of rainfall.

The estimated mean values are used to implement the simulations, i.e., the multifractal parameters are considered to be constant values. The average histograms of the parameters α and C_1, estimated over all the rain periods extracted from a 1002 year long simulated time series, are also shown in Figure 2. The shapes of the α and C_1 distributions estimated from simulated rain periods are quite close to those estimated from real measurements of rain. The average (mean, standard deviation, skewness, and kurtosis) values for the parameter α are found to be close to those estimated from the measured data. However, the average distribution of the parameter C_1 for simulated series has a higher kurtosis, suggesting a heavier tail distribution. Similarly, the mean value of C_1 estimated from simulations (i.e., average mean) is greater (0.12) than that estimated from observations (0.1). Since the distribution of the parameters estimated from data simulated with fixed parameters is similar to that obtained from observed data, we can assume that the observed spread over these constant values may be a consequence of estimation errors (stained among others by the limited size of the samples/rain periods). This justifies the choice of constant parameters.

Assumption 2 is validated, since a multifractal behavior is observed in the data corresponding to within-rain periods. However, as there is no consensus on the estimation of parameters characterizing multifractality, a certain degree of uncertainty remains concerning the exact values of the parameters to be retained.

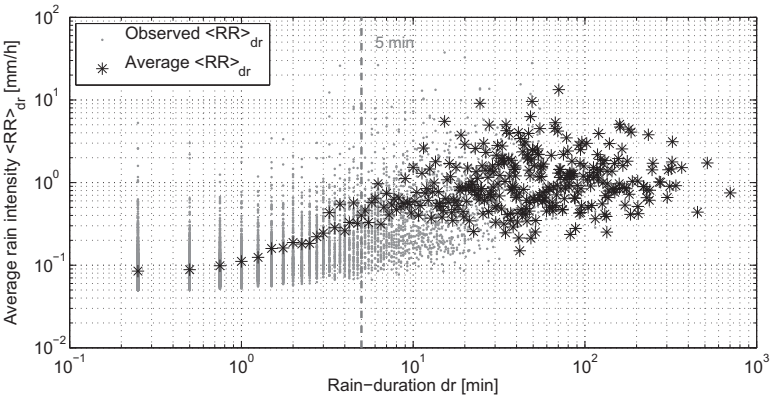


Figure 3. Average rain rate of rain periods $\langle RR\rangle_{d_r}$ as a function of rain duration d_r, over all the rain periods of the training measured time series (2 years DBS time series).

4.3. Rain Period by Rain-Period Denormalizing Parameters (Assumption 3)

At this stage, we are able to generate normalized rain periods corresponding to continuous series of normalized rain rates (RR_N) of known duration d_r. In the following, we examine the usefulness of the rain duration d_r for the retrieval of the corresponding average rain rate (knowing the duration d_r), $\langle RR\rangle_{d_r}$. In Figure 3, two behaviors can be observed. When d_r is shorter than 5 min, a relationship between the average rain rate $\langle RR\rangle_{d_r}$ and the duration could be distinguished, whereas when d_r is greater than 5 min, no significant trend is observed. An approach similar to the particularly attractive method proposed by *De Michele and Salvadori* [2003] could be used, in which, an intensity-duration model using a 2-Copula, is combined with a Generalized Pareto. As our data set did not reveal any clear relationship for durations in excess of 5 min, we chose not to use this approach.

As described by *Menabde and Sivapalan* [2000], the values of $\langle RR\rangle_{d_r}$, corresponding to d_r, greater than 5 min, are drawn in accordance with an alpha-stable distribution (determined by its characteristic function—see equation (7)), while assuming there is no dependence between $\langle RR\rangle_{d_r}$ and the corresponding value of d_r (given $d_r > 5$ min). This hypothesis is consistent with our data set and does not go any further. In the present case, it was found that $\alpha_r \neq 1$ (see Table 2). Since α_r is not equal to unity, in the following we provide the expression for the corresponding alpha-stable characteristic function only:

$$\varphi\left(\langle RR\rangle_{d_r}|\alpha_r,\beta,\gamma,\delta\right)=\exp\left[-\gamma^{\alpha_r}|\langle RR\rangle_{d_r}|^{\alpha_r}\left(1-i\beta tan\left(\frac{\pi\alpha_r}{2}\right)\right)+i\,\delta\langle RR\rangle_{d_r}\right]\ \text{for}\ \alpha_r\neq 1 \tag{7}$$

where $\alpha_r \in]0,2]$ is the stability parameter and describes the tail of the distribution, $\beta \in [-1,1]$ is the skewness parameter, $\gamma \in]0,+\infty[$ is the scale parameter, and $\delta \in]-\infty,+\infty[$ is the location parameter.

In the case where d_r is less than 5 min, taking the relationship $\langle RR\rangle_{d_r}=f(d_r)$ into account does not demonstrate its relevance. Then, $\langle RR\rangle_{d_r}$ is also drawn using an alpha-stable distribution assuming there is no dependence between $\langle RR\rangle_{d_r}$ and the corresponding value d_r (given $d_r < 5$ min). Finally, we draw $\langle RR\rangle_{d_r}$ while considering two different sets of parameters, depending on whether d_r is greater or less than 5 min. As the $\langle RR\rangle_{d_r}$ distribution is highly asymmetric, the parameter β is set to 1, and the value of δ is set to 0, since the average rain intensities are strictly positive values (and hence greater than 0). The only remaining parameters to be determined are α_r and γ. The values of the estimated parameters are shown in Table 2.

Table 2. Parameters of the Conditional (Average Rain Rate $\langle RR\rangle_{d_r}$) Alpha-Stable Distribution Knowing the Rain Duration d_r

Rain Duration Lasting Less Than 5 min				Rain Duration Lasting 5 min or More			
α_r	β	γ	δ	α_r	β	γ	δ
0.90	1	0.01	0	0.77	1	0.16	0

One of the specificities of this study is its use of a finely resolved data set (15 s resolution). Our definition of rain duration (a set of consecutive, 15 s nonzero rain rates) has various implications. When compared to other sensors, we may have an increased number of short rain periods, and therefore a lower number of medium/long rain periods. In practice, our

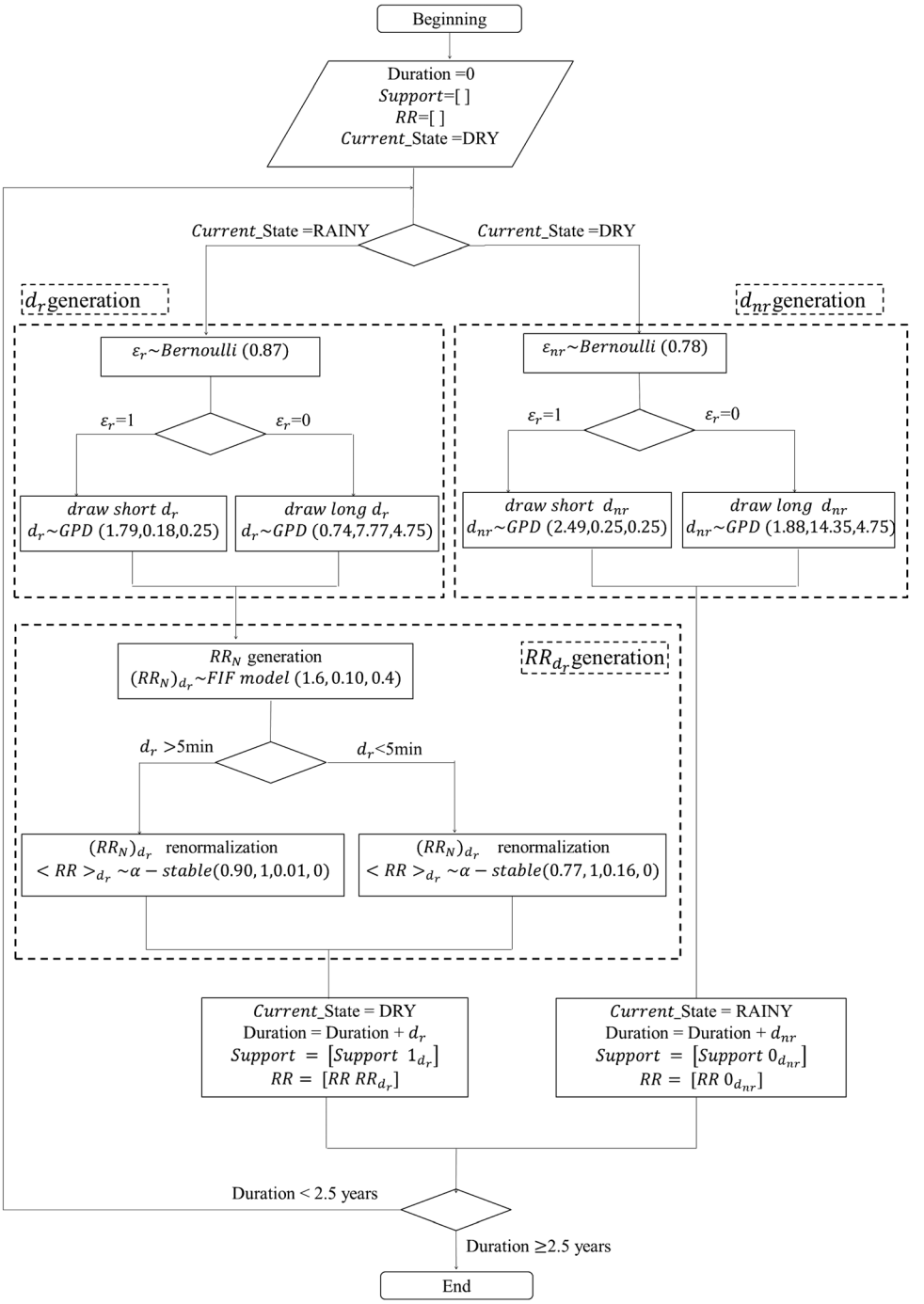


Figure 4. Scheme of the simulation process.

definition of a rain period generally corresponds to portion of what is usually referred to as a rain event. Thus, in a certain sense, we split up single rain events and shuffle the resulting parts before establishing a relationship between $\langle RR \rangle_{d_r}$ and d_r. This process is inherent to the fine-resolution modeling of rain and allows rain rates resulting from a short burst of raindrops to be simulated.

As further discussed in section 5.1, Figure 7c compares the water height Empirical Survival Functions (ESF), obtained for 100 simulated time series at the finest resolution, with the two observed ones. This allows us to validate the third assumption.

4.4. The Simulator

In this section, we provide a detailed description of the simulator (also presented in the scheme in Figure 4). The simulation procedure consists in the following two main steps:

Step 1: Simulation of the rain support.

As previously mentioned, no-rain durations (d_{nr}) and rain durations (d_r) are independent. The rain support is thus obtained by alternating rain and no-rain durations until the simulated time series reaches the desired length. The short (<5 min) or long (>5 min) values of d_{nr} and d_r are drawn randomly, in accordance with their expected occurrences, such that each rain or no-rain duration is simulated according to the following procedure:

- Draw a random Bernoulli variable ϵ simulating the probability of short d_{nr}/d_r (see Table 1, column 2).
- If $\epsilon = 1$, draw a short d_{nr} or d_r according to a Generalized Pareto law (equation (6)), using the parameters provided in Table 1 (columns 3–5).
- If $\epsilon = 0$, draw a long d_{nr} or d_r according to a Generalized Pareto law (equation (6)), using the parameters provided in Table 1 (columns 6–8).

The d_{nr} and d_r values are rounded to the closest multiple of 15 s.

Step 2: Simulation of the rain periods.

For each rain period of duration d_r, we sequentially implement the FIF model, in order to generate normalized RR_N values and then, by multiplying the RR_N by the randomly drawn $\langle RR\rangle_{d_r}$, apply a denormalization step to obtain the corresponding rain rates RR ($RR = RR_N \times \langle RR\rangle_{d_r}$).

For each rain duration d_r:

- Using the FIF model, generate series of length d_r of RR_N normalized values with the corresponding parameters (α=1.6, C_1=0.1, and H=0.4).
- Draw a stable random value $\langle RR\rangle_{d_r}$, using the appropriate parameters provided in Table 2, to denormalize RR_N and obtain the corresponding RR (and thus the simulated rain period).

The process defined above allows rain-rate time series consistent with our data set to be simulated but is representative of a specific (medium latitude) meteorological region only. However, this process can also be adapted to other regions with different specific properties. The multifractal parameters can be considered to be universal, i.e., characterizing a mean physical relationship within an event. The remaining parameters characterizing the support and the rain duration/average rain-rate relationship can be estimated or drawn based on a physical knowledge (or hypotheses), in order to simulate rain-rate time series in other locations governed by different climatic conditions.

5. Characteristics of the Simulated Times Series

At this stage, the simulator has been partially validated by systematically controlling each hypothesis of the model. The next step involves additional controls, through the investigation of various properties of the entire rain-rate time series. This also allows us to check the model's ability to restore rain properties that are not directly used in the model. In this section, in order to assess the correct behavior of the simulator, we used 100 simulated time series having a 2.5 year duration and 15 s resolution. These were then compared with the two original time series (see section 2).

5.1. Scaling Properties of Rain Series

To illustrate the simulator's ability to generate realistic rainfall time series, we studied the fractal properties of the 100 simulated rain supports. In various studies, the rain support is assumed to be fractal. This is one of the reasons for which *Over and Gupta* [1996], *Schmitt et al*. [1998], *Serinaldi* [2010], *Veneziano et al*. [2006], and *Veneziano and Lepore* [2012] (among others) used the beta model to generate rain supports. This property implies that the rain support behaves according to the following relationship:

$$Pr(RR_\lambda > 0) \propto \lambda^{-C_f} \tag{8}$$

where λ denotes the resolution, C_f denotes the codimension, and RR_λ is the rain rate at scale λ. To validate the rain support simulation, it is also necessary to verify that the fractal nature of the resulting support is

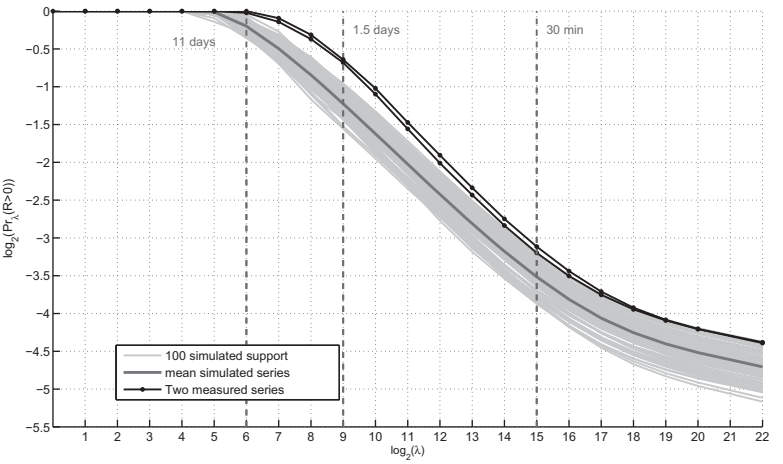


Figure 5. Probability of rain occurrence at a given resolution $Pr(RR_\lambda > 0)$ for the two measured time series (black solid + circle) and for a 100 simulated 2 year rain supports (grey lines) as a function of resolution λ. The average of the 100 simulated $Pr(RR_\lambda > 0)$ curves is also shown (dark grey).

preserved. Figure 5 shows the probability of rain occurrence $(Pr(RR_\lambda > 0))$, for a given resolution λ. This relationship is shown on a log-log scale. The rain occurrence of the two measured rain supports (black solid curve), as well as the occurrences of the 100 simulated supports (grey curves), is characterized by fractal behavior between the scales $\lambda = 2^{15}$ and $\lambda = 2^9$ (corresponding to time scales ranging between 30 min and 1.5 days). The linear behavior of this log-log plot corresponds to fractal behavior, between 30 min and 1.5 days, for both the measured and simulated supports. The slopes of the log-log fits to the two measured time series correspond to estimated codimensions C_f equal to 0.42 and 0.41, respectively (see Table 3), whereas the 100 simulated supports lead to a mean value of 0.38. The simulated and measured codimensions are thus very close.

The 100 simulated supports (at 15 s) have a mean probability of rain occurrence equal to 3.85% as opposed to the values of 4.6% and 5.31% observed for the two measured rain supports. Although the slopes of the linear portion are rather similar, there is nevertheless a noticeable offset between the two plots. At the finer resolution ($\lambda = 2^{22}$, corresponding to an integration time of 15 s), the two (black) measured curves lie above the 100 (grey) simulated curves. The simulated $Pr(RR_\lambda > 0)$ is lower than expected. This implies a lack of rain support (or an excess of zeros/no-rain periods). For fine scales (from $\lambda = 2^{22}$ to $\lambda = 2^{12}$), apart from an offset, all of the curves are similar in shape.

The offset between simulations and measurements can be explained by an excess of longer no-rain d_{nr} durations. As it can be seen (see Figure 1), there is a tendency to slightly over sample the simulated long no-rain d_{nr} durations. In Figure 5, for $\lambda = 2^6$ (corresponding to approximately 11 days), whereas the two observed curves reach the value 0 (probability of rain occurrence = 1, at resolution λ) the dark grey curve representing the average values of the simulated curves does not reach this value. This outcome means that the model is able to simulate no-rain durations d_{nr} that can be longer (or slightly more frequent) than those measured during real observations. It explains the offset found at the resolution $\lambda = 2^6$ as well as at finer scales (until resolution $\lambda = 2^{22}$). This comparison between the properties of simulated/measured rain supports provides a posteriori validation of the relevance of assumption 1. Furthermore, it is

Table 3. Codimension and Percentage of Rain Estimated for the Two Measured Time Series (Columns 2 and 3)[a]

	Observed DBS Series		100 Simulated Series			
			Mean	Q_1	Q_2	Q_3
Codimension	0.42	0.41	0.38	0.39	0.38	0.37
Percentage of rain	4.6	5.31	3.85	3.51	3.85	4.15

[a]Mean, first, second, and third quartiles (columns 4–7) of the codimension and the percentage of rain (at the finer resolution), estimated for the corresponding 100 simulated time series.

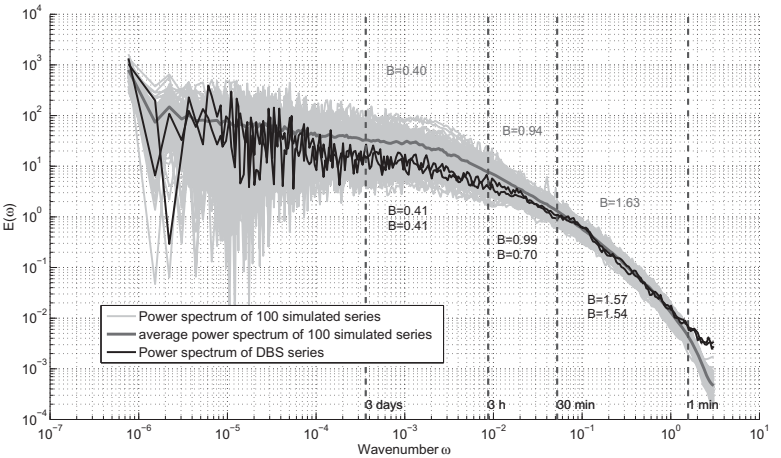


Figure 6. Power spectra of the two measured time series (thin, black) and average power spectrum (thick, dark grey), computed from a 100 simulated time series spectra (also indicated by light grey).

important to notice that for measurements with a resolution finer than 30 min, the scaling behavior of the support is broken. In this case, a disaggregation model based on a monofractal cascade would not function correctly. Here since there is no scaling of the support under 30 min, a beta-log-stable UM model (coarsely a multifractal process generated over a fractal support) would not provide a correct distribution of rain occurrences for resolutions finer than 30 min. For this kind of UM model, the rain support can influence the multifractal parameter estimation (through an inappropriate mixing of rain support and "within-rain" properties).

Figure 6 provides a log-log plot of the power spectra of the two measured time series, and of the 100 simulated time series. The average spectrum is also shown (wide, dark grey line). While reproducing a certain variability (light grey area), the mean spectrum of the 100 simulated time series is consistent with measurements. We can only hope that the measurements behave as a sample among the others, which they do. Indeed, for the full time span covered by these time series, the corresponding spectra have similar scaling factors, over coherent time scales. As reported in previous studies [e.g., *Fraedrich and Larnder*, 1993; *Tessier et al*., 1996; *De Montera et al*., 2009; *Schertzer and Lovejoy*, 2011; *Verrier et al*., 2011], the scaling properties between 1 min and 3 days are analyzed by partitioning the full range into a set of different scaling regimes. The scaling regime corresponding to more than 3 days is strictly due to the rain support, and that equal to 30 min characterizes within-rain periods, the central part of which corresponds to a transition stage. These scaling regimes are characterized by the slope value B, which is used rather than the traditional β, to avoid confusion with β used here to indicate the stable characteristic function of equation (7).

The "within-rain" slopes (1−30 min) of the simulated power spectra have a value >1, indicating a nonconservative field; this is thus consistent with the parameter H, which is equal to 0.4. The slope B of the mean spectra is found to be equal to 1.63 (see Table 4), which is very close to the two values estimated from the measured DBS series (1.57 and 1.54, respectively).

The scaling properties introduced by the simulation of rain periods (generally <30 min) clearly explain the first slope (for time scales shorter than 30 min) resulting from the use of the FIF model. The consistency of the scaling properties obtained for the entire time span (Table 4) necessarily results from the rain support properties (for time scales greater than 30 min). In other words, from a spectral point of view, the good agreement between the measurements and the simulations validates the rain support simulation (independent rain/no-rain durations: assumption 1), as well as the within-rain-period simulation (rain-rate series simulated with the FIF model: assumption 2).

In this subsection, it has been shown that the rain support influences the power spectrum in the case of low frequencies (periods longer than 30 min), and that care should be taken when estimating/explaining scaling properties over such periods of time.

Table 4. Slope of the Power Spectrum Obtained With the Two Measured Time Series for the Three Scaling Regimes (Line 2)[a]

	B in Scaling Regime 1 min → 30 min				*B* in Scaling Regime 30 min → 3 h				*B* in Scaling Regime 3 h → 3 days			
DBS series	1.57				0.99				0.41			
	1.54				0.70				0.41			
	Mean	Q_1	Q_2	Q_3	Mean	Q_1	Q_2	Q_3	Mean	Q_1	Q_2	Q_3
100 simulated series	1.63	1.57	1.62	1.66	0.94	0.74	0.93	1.10	0.40	0.22	0.39	0.48

[a]Mean, first, second, and third quartiles of the slope estimated for the 100 simulated spectra for three different scaling regimes.

5.2. More Classical Properties of Rain

Beyond the multifractal properties of rain, it is important to verify that the simulated time series are consistent with the behavior that could normally be expected with rainfall. It is commonly studied through the Empirical Survival Function (ESF hereafter). Since we are dealing with rain periods rather than rain events, the ESF is computed for three characteristic quantities: rain rates *RR*, rain duration d_r, and rain-duration water heights (referred to as water height in the following). It is important to verify that the scaling properties do in practice lead to simulated time series that are consistent with measurements made at coarser resolutions. This can be assessed by aggregating all the 15 s time series, to obtain the ESF at four commonly used time resolutions (5 min, 1 h, and 1 day). As shown in the previous section, we use the two measured time series, as well as the 100 simulated time series (spanning 2.5 years), with a resolution of 15 s.

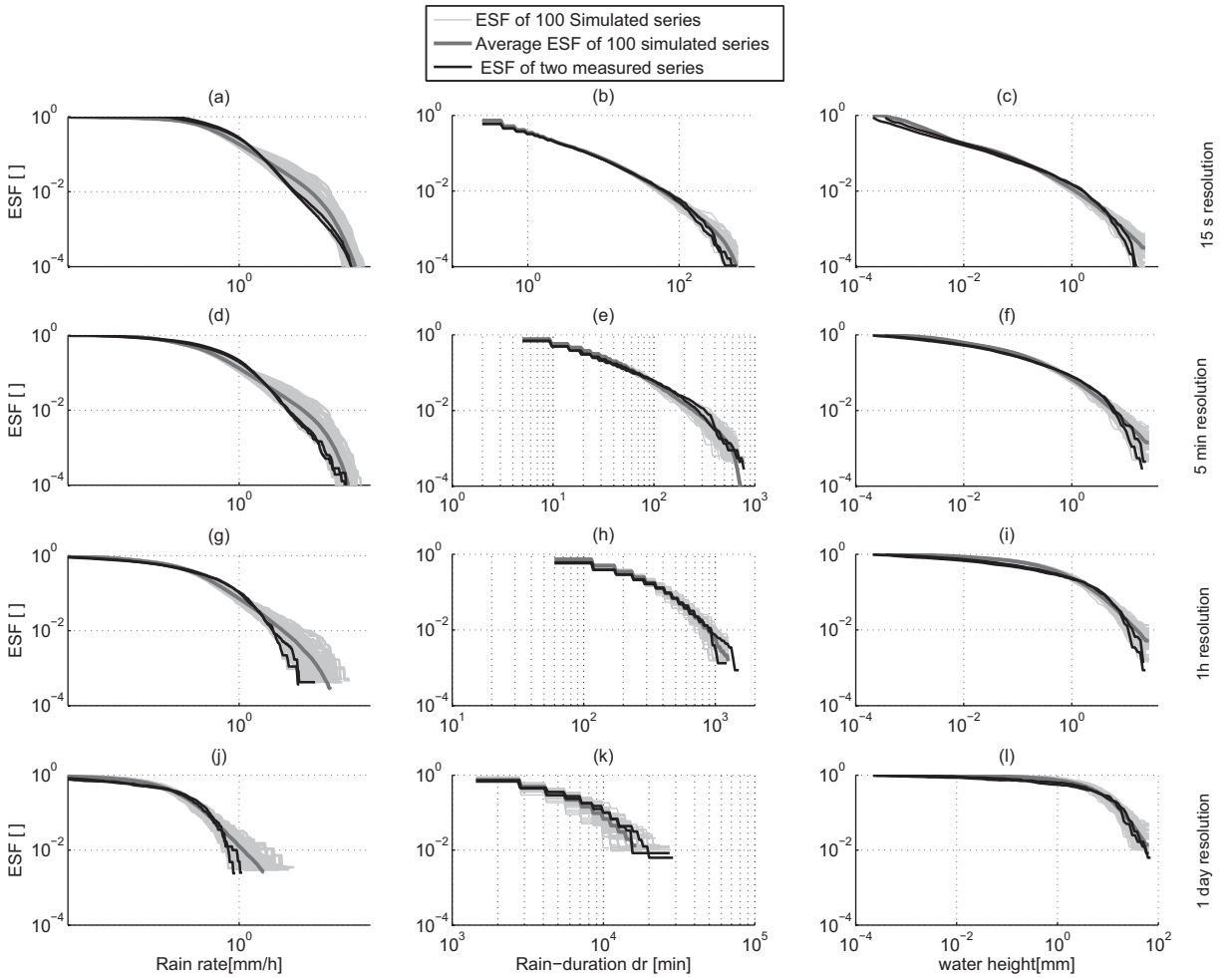


Figure 7. (left to right) Empirical Survival Functions of rain rates *RR*, rain durations *d*, (i.e., length of consecutive nonzero rain rates), and the (corresponding) water height. (top to bottom) The ESFs are shown for the high-resolution series (15 s), and for the 5 min, 1 h, and 1 day aggregated series.

For each plot shown in Figure 7, we have drawn the ESF curves corresponding to the measured time series (the two black curves), and the curves representing the 100 simulated time series (light grey curves), together with the mean value of the latter (dark grey curve). Each row of plots in Figure 7 corresponds to the same value of resolution, shown in the right of the figure, and each column corresponds to a rain property indicated at the bottom of the figure. The plots shown in the first row thus correspond to the finest, 15 s resolution (i.e., that used for the measurements and the simulations). The plots in the other three rows show the aggregated ESFs of the simulated or measured 15 s time series, corresponding to coarser temporal resolutions (5 min, 1 h, and 1 day).

This figure shows that the ESF computed from simulated data still remains in agreement with those obtained from measured data, which means that temporal scale relations and rain intermittency are well represented in our model. From that perspective, it is reasonable to consider the measured time series as a representative realization of the simulation process. The good behavior of the aggregated series (at all different resolutions) validates the simulator's ability to generate coherent time series, for all values of temporal resolution. As expected, larger values are characterized by a stronger variability, due to their lower frequency of occurrence. The occurrence of extreme values is thus in agreement with the measurements and hypotheses used to build the model.

The rain-duration plots shown in the second column (Figures 7b, 7e, 7h, and 7k) confirm the information revealed in Figure 5. This provides a different way of viewing the rain support, and validates assumption 1. Despite its tendency to slightly overestimate the short durations, the simulated rain-duration ESFs are very close to the two measured ESFs. For larger values, a difference can be noted between the behaviors of the rain-duration ESFs. A slight bend can also be seen in one of the measured curves in Figure 7e—as previously discussed, this type of effect can be accounted for by the natural variability of the simulation.

The ESFs shown as a function of rain-duration water height in the third column (Figures 7c, 7f, 7i, and 7l) are proportional to the product of the rain duration and the average rain rate: $\langle RR \rangle_{d_r} . d_r$. Since the consistence of the simulated rain support has been demonstrated, this can provide an additional method for validation of the relationship between $\langle RR \rangle_{d_r}$ and d_r (assumption 3). Although the 15 s ESFs corresponding to the mean of the 100 simulations are not as smooth as the original ESFs, the simulations show that these are consistent with the measurements. When 2 year time series and their aggregated counterparts are considered, there is no apparent consequence in term of the dependencies that may have been suppressed by the simulation process between other rain characteristics.

The four rain-rate plots shown in the first column (Figures 7a, 7d, 7g, and 7j) represent rain-rate ESFs. These result from the combined use of our three assumptions, and it can be seen that there is also a good correspondence between the measured and simulated ESFs at all resolutions.

As a result, Figure 7 shows that the simulated time series provide a very good representation of the information contained in the originally measured data (two series of 2 year periods), at several commonly used resolutions. A more thorough investigation accounting for seasonal trends and long-range dependences will be investigated when these data become available. Nevertheless, the simulator could be run over longer time spans, in order to study the occurrence of potentially extreme values, and their corresponding return periods.

6. Conclusion and Discussion

Guided by previous studies [*Lavergnat and Golé*, 1998, 2006; *De Montera et al*., 2009, 2010; *Verrier et al*., 2010, 2011], the main objective of this research has been to simulate rain time series with statistical properties (distribution and scaling invariance) representative of a particular climatic region. Our methodology is based on two main steps, namely the simulation of rain support, and of realistic rain rates. These steps are based on several important hypotheses, relying mainly on the high resolution of the data set. These supporting hypotheses are thoroughly validated. The originality of this study is that a very good agreement is established between measurements and simulations, for a significant number of properties that coherently characterize rain. When necessary, the validation was systematically run over the full time series, rather than for selected events only. The resulting simulated fine-resolution time series incorporates information that is coherent with the various time scales of the original measurements. When aggregated over a duration of

up to 1 day, the simulated time series preserves its coherent features (rain-rate distributions in particular) at various resolutions.

This study shares similarities with other studies, such as that of *Veneziano and Lepore* [2012], dealing with the simulation of time series with scaling properties. The difference in resolution between our measurements (15 s resolution) and those used in the aforementioned study (1 h resolution) explains some of the apparent discrepancies. As previously discussed and demonstrated by *Veneziano and Lepore* [2012], we emphasize the importance of rain support and explain how this can introduce a bias into the estimated multifractal parameters. As described in section 3.2, the fine resolution of the time series allows the influence of the rain's intermittency (zero of the rain support) on the rain-rate values to be cancelled. This corroborates assumption 2, namely the independence of rain support properties with respect to the multifractal/scaling of within-rain parameters. Our model successfully retrieves a simulated power spectrum (Figure 6) showing scaling breaks consistent with the original data set. This is not commonly achieved with standard UM models. Although our study does not focus on the retrieval of multifractal parameters, we can try to discuss this. As a consequence of their coarse time resolution, rain gauges do not allow within-event rain-rate scaling properties to be correctly discriminated from intermittency. Since numerous multifractal models are based on parameters estimated through the processing of rain gauge time series, the extensive set of parameters (some of which are presented at the end of section 4.2) can be explained by this mixing. *De Montera et al*. [2009] showed that coherent multifractal parameters are found in three different climatic regions. We believe that this set of parameters could be universal or at least considerably reduced through the use of fine-resolution sensors. In other words, as suggested by *Gires et al*. [2013], we believe that these parameters vary from one geographical location to another through the zero values of the various rain supports. Among others, *Veneziano and Lepore* [2012] determined a value of 2 for parameter α, whereas our study led to a value of 1.6. Since their measurements are integrated over 1 h, they can be considered to smooth out the rain rate. Indeed, the 1 h measurements result from mixing fine-resolution rain periods with fine-resolution zeros (corresponding to the no-rain durations). This interpretation would explain the greater value of α characterizing less sparse time series (less small values and less spikes).

Although rain event modeling is considered to be universal, the parameters describing rain support and rain duration/average rain-rate relationship can fluctuate from one geographical area to another. The use of parametric methods, associated with reasonable hypotheses and expert knowledge, can be very beneficial. Finally, it is important to note that there is a relatively high cost associated with the design and development of a simulator with characteristics (and especially those of rain support) close to those of the "real world." Indeed 25 parameters were represented: 14 to model the rain support, 3 to represent the within-rain variability, and 8 for the denormalization process. However, among these parameters, some have fixed values and some others are not expected to change significantly. Indeed, if it is assumed that short durations and within-rain parameters result from the laws of physics governing rain, the parameter requirement could be simplified by the following: eight parameters for rain support modeling and three FIF parameters could be considered as "global" or "universal." Four of the rain duration/average rain rate relationship parameters are fixed, whatever the climatic region (due mainly to the positivity of the rain rate). As the four remaining parameters related to the duration/average rain-rate relationship were not studied with another data set, it is currently difficult to gain a clear understanding of their variability. Finally, at maximum of 10 parameters need to be evaluated, in order to adapt the simulator to a different climatic region. Ideally, a time series with a 15 s resolution would be required to correctly estimate these. However, they could, in practice, be estimated from a series with coarser resolution. Typically, a 1 or 5 min time series should suffice, since the within-rain properties are not expected to change significantly from one place to another.

A question can be raised on the specific behavior for the rain support below 5 min identified in this work. Could this behavior be common to all rain events, whatever the location?

In principle, this simulation/validation approach could be applied to other fine-resolution time series. As rain modeling is considered to vary from one location to another, some of our hypotheses and parameters could be expected to vary. Thus, to improve the modeling of rainfall at different geographic locations, it would be helpful to have an improved understanding of their differences and/or similarities.

In view of the limited time span covered by our time series (2 years), it is not possible to draw special attention to the seasonality of the results. Furthermore, we were able to use a coarse resolution relationship only,

between the average rain rate and the rain duration. To improve these aspects of our model, it would be necessary we need to study a longer time series. As we do not currently have longer fine-resolution time series, it would be useful to compare our results with those obtained using other sensors for which longer series are available. An intercomparison of sensors (typically the DBS and a conventional tipping bucket rain gauge) would allow us to gain a better understanding of the influence of the sensor's resolution and sensitivity on the accuracy of rain property retrieval. At a resolution coarser than 1 h, although both the rain gauge and the DBS disdrometer give consistent water volumes, discrepancies appear when finer resolutions are considered. A better understanding of this should help us improve the simulator and/or test its accuracy over longer periods of time. This would lead to longer simulated series, and thus give access to statistics over longer time spans (providing information, on less frequent extreme events). The study of series over longer periods of time may contribute toward emphasizing any seasonal trend in the rain series. It could also invalidate the independence of no-rain and rain durations, and therefore lead to enhanced modeling of the rain support.

Acknowledgments

The authors thank the two reviewers who contributed their judicious and helpful remarks. This study was partially supported by the French "Programme National de Télédétection Spatiale" (PNTS, http://www.insu.cnrs.fr/actions-sur-projets/pnts-programme-national-de-teledetection-spatiale), grant PNTS-2013-01. The data set used in this study is available, on demand, from the authors.

References

Bernardara, P., C. De Michele, and R. Rosso (2007), A simple model of rain in time: An alternating renewal process of wet and dry states with a fractional (non-Gaussian) rain intensity, *Atmos. Res.*, *84*(4), 291–301.

Burton, A., C. Kilsby, H. Fowler, P. Cowpertwait, and P. O'Connell (2008), RainSim: A spatial–temporal stochastic rainfall modelling system, *Environ. Modell. Software*, *23*(12), 1356–1369.

Cooley, D., D. Nychka, and P. Naveau (2007), Bayesian spatial modeling of extreme precipitation return levels, *J. Am. Stat. Assoc.*, *102*(479), 824–840.

De Michele, C., and M. Ignaccolo (2013), New perspectives on rainfall from a discrete view, *Hydrol. Processes*, *27*(16), 2379–2382.

De Michele, C., and G. Salvadori (2003), A generalized pareto intensity-duration model of storm rainfall exploiting 2-copulas, *J. Geophys. Res.*, *108*(D2), 4067, doi:10.1029/2002JD002534.

De Montera, L., L. Barthès, C. Mallet, and P. Golé (2009), The effect of rain-no rain intermittency on the estimation of the universal multifractals model parameters, *J. Hydrometeorol.*, *10*(2), 493–506.

De Montera, L., S. Verrier, C. Mallet, and L. Barthès (2010), A passive scalar-like model for rain applicable up to storm scale, *Atmos. Res.*, *98*(1), 140–147.

Deidda, R. (2000), Rainfall downscaling in a space-time multifractal framework, *Water Resour. Res.*, *36*(7), 1779–1794.

Deidda, R., R. Benzi, and F. Siccardi (1999), Multifractal modeling of anomalous scaling laws in rainfall, *Water Resour. Res.*, *35*(6), 1853–1867.

Delahaye, J.-Y., L. Barthès, P. Golé, J. Lavergnat, and J.-P. Vinson (2006), A dual-beam spectropluviometer concept, *J. Hydrol.*, *328*(1), 110–120.

Evin, G., and A.-C. Favre (2013), Further developments of a transient Poisson-cluster model for rainfall, *Stochastic Environ. Res. Risk Assess.*, *27*(4), 831–847.

Fraedrich, K., and C. Larnder (1993), Scaling regimes of composite rainfall time series, *Tellus, Ser. A*, *45*(4), 289–298.

Gaume, E., N. Mouhous, and H. Andrieu (2007), Rainfall stochastic disaggregation models: Calibration and validation of a multiplicative cascade model, *Adv. Water Resour.*, *30*(5), 1301–1319.

Gires, A., I. Tchiguirinskaia, D. Schertzer, and S. Lovejoy (2012), Influence of the zero-rainfall on the assessment of the multifractal parameters, *Adv. Water Resour.*, *45*, 13–25.

Gires, A., I. Tchiguirinskaia, D. Schertzer, and S. Lovejoy (2013), Development and analysis of a simple model to represent the zero rainfall in a universal multifractal framework, *Nonlinear Processes Geophys.*, *20*, 343–356, doi:10.5194/npg-20-343-2013.

Hubert, P. (2001), Multifractals as a tool to overcome scale problems in hydrology, *Hydrol. Sci. J.*, *46*(6), 897–905.

Ignaccolo, M., and C. De Michele (2010), A point based Eulerian definition of rain event based on statistical properties of inter drop time intervals: An application to Chibolton data, *Adv. Water Resour.*, *33*(8), 897–905.

Lavallée, D., S. Lovejoy, and D. Schertzer (1993), Nonlinear variability and landscape topography: Analysis and simulation, in *Fractals in Geography*, edited by L. De Cola and N. Lam, pp. 158–192, Prentice Hall, Englewood Cliffs.

Lavergnat, J., and P. Golé (1998), A stochastic raindrop time distribution model, *J. Appl. Meteorol.*, *37*(8), 805–818.

Lavergnat, J., and P. Golé (2006), A stochastic model of raindrop release: Application to the simulation of point rain observations, *J. Hydrol.*, *328*(1), 8–19.

Leblois, E., and J.-D. Creutin (2013), Space-time simulation of intermittent rainfall with prescribed advection field: Adaptation of the turning band method, *Water Resour. Res.*, *49*, 3375–3387, doi:10.1002/wrcr.20190.

Lovejoy, S., and D. Schertzer (1995), Multifractals and rain, in *New Uncertainty Concepts in Hydrology and Hydrological Modelling*, edited by Z. W. Kundzewicz, pp. 62–103, Cambridge Univ. Press, Cambridge.

Lovejoy, S., and D. Schertzer (2008), Turbulence, raindrops and the l1/2 number density law, *New J. Phys.*, *10*(7), 075017.

Lovejoy, S., and D. Schertzer (2010), On the simulation of continuous in scale universal multifractals, Part i: Spatially continuous processes, *Comput. Geosci.*, *36*(11), 1393–1403.

Lovejoy, S., D. Schertzer, and V. Allaire (2008), The remarkable wide range spatial scaling of TRMM precipitation, *Atmos. Res.*, *90*(1), 10–32.

Menabde, M., and M. Sivapalan (2000), Modeling of rainfall time series and extremes using bounded random cascades and levy-stable distributions, *Water Resour. Res.*, *36*(11), 3293–3300.

Molini, A., G. G. Katul, and A. Porporato (2009), Revisiting rainfall clustering and intermittency across different climatic regimes, *Water Resour. Res.*, *45*, W11403, doi:10.1029/2008WR007352.

Novikov, E., and R. Stiuart (1964), The intermittency of turbulence and the spectrum of energy dissipation, *Izv. Geophys. Ser*, *3*, 408–413.

Olsson, J. (1998), Evaluation of a scaling cascade model for temporal rain-fall disaggregation, *Hydrol. Earth Syst. Sci.*, *2*, 19–30.

Onof, C., R. Chandler, A. Kakou, P. Northrop, H. Wheater, and V. Isham (2000), Rainfall modelling using Poisson-cluster processes: A review of developments, *Stochastic Environ. Res. Risk Assess.*, *14*(6), 384–411.

Over, T. M., and V. K. Gupta (1996), A space-time theory of mesoscale rainfall using random cascades, *J. Geophys. Res.*, *101*(D21), 26,319–26,331.

Pathirana, A., S. Herath, T. Yamada, et al. (2003), Estimating rainfall distributions at high temporal resolutions using a multifractal model, *Hydrol. Earth Syst. Sci. Discuss.*, *7*(5), 668–679.
Pecknold, S., S. Lovejoy, D. Schertzer, C. Hooge, and J. Malouin (1993), The simulation of universal multifractals., in *Cellular Automata: Prospects in Astronomy and Astrophysics*, edited by J. M. Perdang and A. Lejeune, vol. 1, pp. 228–267, World Sci., Singapore.
Rodríguez, R., M. Casas, and A. Redaño (2013), Multifractal analysis of the rainfall time distribution on the metropolitan area of Barcelona (Spain), *Meteorol. Atmos. Phys.*, *121*(3–4), 181–187.
Rupp, D. E., R. F. Keim, M. Ossiander, M. Brugnach, and J. S. Selker (2009), Time scale and intensity dependency in multiplicative cascades for temporal rainfall disaggregation, *Water Resour. Res.*, *45*, W07409, doi:10.1029/2008WR007321.
Schertzer, D., and S. Lovejoy (1987), Physically based rain and cloud modeling by anisotropic, multiplicative turbulent cascades, *J. Geophys. Res*, *92*(D8), 9693–9714.
Schertzer, D., and S. Lovejoy (1991), Nonlinear geodynamical variability: Multiple singularities, universality and observables, in *Non-Linear Variability in Geophysics*, pp. 41–82, Springer, Netherlands.
Schertzer, D., and S. Lovejoy (2011), Multifractals, generalized scale invariance and complexity in geophysics, *Int. J. Bifurcation Chaos*, *21*(12), 3417–3456.
Schertzer, D., S. Lovejoy, and P. Hubert (2002), An introduction to stochastic multifractal fields, in *ISFMA Symposium on Environmental Science and Engineering With Related Mathematical Problems*, pp. 106–179, Higher Educ. Press, Beijing.
Schleiss, M., A. Berne, and R. Uijlenhoet (2009), Geostatistical simulation of 2d fields of raindrop size distributions at the meso-scale, *Water Resour. Res.*, *45*, W07415, doi:10.1029/2008WR007545.
Schleiss, M., S. Chamoun, and A. Berne (2014), Stochastic simulation of intermittent rainfall using the concept of "dry drift," *Water Resour. Res.*, *50*, 2329–2349, doi:10.1002/2013WR014641.
Schmitt, F. (2014), Continuous multifractal models with zero values: A continuous β-multifractal model, *J. Stat. Mech. Theory Exp.*, *2014*(2), P02008.
Schmitt, F., S. Vannitsem, and A. Barbosa (1998), Modeling of rainfall time series using two-state renewal processes and multifractals, *J. Geophys. Res.*, *103*(D18), 23,181–23,193.
Serinaldi, F. (2010), Multifractality, imperfect scaling and hydrological properties of rainfall time series simulated by continuous universal multifractal and discrete random cascade models, *Nonlinear Processes Geophys.*, *17*, 697–714, doi:10.5194/npg-17-697-2010.
Tessier, Y., S. Lovejoy, and D. Schertzer (1993), Universal multifractals: Theory and observations for rain and clouds, *J. Appl. Meteorol.*, *32*(2), 223–250.
Tessier, Y., S. Lovejoy, P. Hubert, D. Schertzer, and S. Pecknold (1996), Multifractal analysis and modeling of rainfall and river flows and scaling, causal transfer functions, *J. Geophys. Res.*, *101*(D21), 26,427–26,440.
Tyralis, H., and D. Koutsoyiannis (2011), Simultaneous estimation of the parameters of the Hurst–Kolmogorov stochastic process, *Stochastic Environ. Res. Risk Assess.*, *25*(1), 21–33.
Vainshtein, S. I., K. R. Sreenivasan, R. T. Pierrehumbert, V. Kashyap, and A. Juneja (1994), Scaling exponents for turbulence and other random processes and their relationships with multifractal structure, *Phys. Rev. E*, *50*(3), 1823–1835.
Veneziano, D., and C. Lepore (2012), The scaling of temporal rainfall, *Water Resour. Res.*, *48*, W08516, doi:10.1029/2012WR012105.
Veneziano, D., P. Furcolo, and V. Iacobellis (2006), Imperfect scaling of time and space–time rainfall, *J. Hydrol.*, *322*(1), 105–119.
Verrier, S., L. De Montera, L. Barthès, and C. Mallet (2010), Multifractal analysis of African monsoon rain fields, taking into account the zero rain-rate problem, *J. Hydrol.*, *389*(1), 111–120.
Verrier, S., C. Mallet, and L. Barthès (2011), Multiscaling properties of rain in the time domain, taking into account rain support biases, *J. Geophys. Res.*, *116*, D20119, doi:10.1029/2011JD015719.
Wang, Z., M. Schleiss, J. Jaffrain, A. Berne, and J. Rieckermann (2012), Using Markov switching models to infer dry and rainy periods from telecommunication microwave link signals, *Atmos. Meas. Tech.*, *5*(7), 1847–1859.
Yaglom, A. (1966), The influence of fluctuations in energy dissipation on the shape of turbulence characteristics in the inertial interval, in *Soviet Physics Doklady*, vol. 11, p. 26–29.

Erratum

In the originally published version of this article, incorrect affiliations were listed for the authors. The affiliations have since been corrected, and this version may be considered the authoritative version of record.